

# Maximal energy that can be converted by a dielectric elastomer generator

Soo Jin Adrian Koh<sup>1,2</sup>, Xuanhe Zhao<sup>2</sup> and Zhigang Suo<sup>2,a</sup>

*<sup>1</sup>Institute of High Performance Computing  
1 Fusionopolis Way, #16-16 Connexis, Singapore 138632, Singapore*

*<sup>2</sup>School of Engineering and Applied Sciences, Harvard University  
Cambridge, Massachusetts 02138, USA*

## Abstract

Mechanical energy can be converted to electrical energy by using a dielectric elastomer generator. The elastomer is susceptible to various modes of failure, including electrical breakdown, electromechanical instability, loss of tension, and rupture by stretch. The modes of failure define a cycle of maximal energy that can be converted. This cycle is represented on planes of work-conjugate coordinates, and may be used to guide the design of practical cycles.

<sup>a</sup>email: [suo@seas.harvard.edu](mailto:suo@seas.harvard.edu)

Diverse technologies are being developed to harvest energy from renewable sources.<sup>1-3</sup> This Letter focuses on one particular technology: dielectric elastomer (DE) generators.<sup>4-8</sup> When a membrane of a dielectric elastomer is pre-stretched and pre-charged, a reduction in the tensile force under the open-circuit condition increases the voltage (Fig. 1). Thus, a cycle can be designed to convert mechanical energy into electrical energy. Experiments have shown that dielectric elastomers can convert energy up to 0.4 J/g, which is at least an order of magnitude higher than the specific energies of piezoelectric ceramics and electromagnetic generators.<sup>5</sup> DE generators have been designed to harvest energy from walking<sup>5,6</sup>, ocean waves<sup>7</sup>, wind and combustion<sup>8</sup>. These generators are lightweight, compliant, and rust-free, allowing them to be deployed widely.

This Letter describes a model to calculate the maximal energy that can be converted by a DE generator. The elastomer is susceptible to various modes of failure.<sup>9,10</sup> We use these modes of failure to define a cycle on the force-displacement plane and the voltage-charge plane. The area enclosed by the cycle gives the maximal energy of conversion. Such a diagram may be used to guide the design of practical cycles.

Our model is based on a nonlinear theory of elastic dielectrics.<sup>11-18</sup> With reference to Fig. 1, consider a membrane of a dielectric elastomer, of sides  $L_1$ ,  $L_2$  and  $L_3$  in its undeformed state. The two faces of the membrane are coated with compliant electrodes. When the electrodes are subject to voltage  $\Phi$  and the membrane is subject to forces  $P_1$  and  $P_2$ , the electrodes gain charges  $+Q$  and  $-Q$ , and the membrane deforms to a state of sides  $\lambda_1 L_1$ ,  $\lambda_2 L_2$  and  $\lambda_3 L_3$ , where  $\lambda_1$ ,  $\lambda_2$  and  $\lambda_3$  are the stretches of the membrane in the three directions. The membrane is taken to be incompressible, so that  $\lambda_1 \lambda_2 \lambda_3 = 1$ . Define the nominal stresses by  $s_1 = P_1 / L_2 L_3$  and  $s_2 = P_2 / L_1 L_3$ , the nominal electric field by  $\tilde{E} = \Phi / L_3$ , and the nominal electric displacement by  $\tilde{D} = Q / L_1 L_2$ . By contrast, the true stresses  $\sigma_1$  and  $\sigma_2$ , the true electric field  $E$ , and the true electric displacement  $D$  are the same quantities divided by the dimensions of the membrane in

the deformed state. The true quantities relate to the nominal ones as  $\sigma_1 = s_1 \lambda_1$ ,  $\sigma_2 = s_2 \lambda_2$ ,  $E = \tilde{E} \lambda_1 \lambda_2$ , and  $D = \tilde{D} \lambda_1^{-1} \lambda_2^{-1}$ .

To illustrate essential ideas, consider the case where the membrane is subject to equal biaxial forces, so that  $s_1 = s_2 = s$  and  $\lambda_1 = \lambda_2 = \lambda$ . The membrane is taken to deform under an isothermal condition, and the temperature will not be considered explicitly. Consequently, the membrane is a thermodynamic system of two independent variations. The variations can be described by two independent variables of many choices. Once chosen, the two independent variables can be used as the coordinates of a plane, and each point in the plane represents a thermodynamic state of the system. To calculate the energy of conversion, we choose planes of work-conjugate coordinates: either the force-displacement plane or the voltage-charge plane (Fig. 2).

We prescribe the equations of state by using the model of ideal dielectric elastomer.<sup>19</sup> The elastomer is a network of polymers with a low density of crosslinks, so that polarization is negligibly affected by deformation. This model has been used almost exclusively in the literature on dielectric elastomers; see Ref. 20 for a review. For an ideal dielectric elastomer subject to a biaxial stress  $s$  and electric field  $\tilde{E}$ , the equations of states are<sup>21</sup>

$$\frac{s}{\mu} = \lambda - \lambda^{-5} - \frac{\tilde{D}^2}{\epsilon\mu} \lambda^{-5}, \quad (1)$$

$$\frac{\tilde{E}}{\sqrt{\mu/\epsilon}} = \frac{\tilde{D}}{\sqrt{\epsilon\mu}} \lambda^{-4}, \quad (2)$$

where  $\mu$  is the modulus, and  $\epsilon$  the permittivity. In numerical calculations, we assume that  $\mu = 10^6 \text{ N/m}^2$  and  $\epsilon = 3.54 \times 10^{-11} \text{ F/m}$ . Using these equations of state, we can map any point in the force-displacement plane to a point in the voltage-charge plane, and vice versa.

When the membrane is uncharged,  $\tilde{D} = 0$  and  $\tilde{E} = 0$ , eq. (1) becomes that

$$\frac{s}{\mu} = \lambda - \lambda^{-5}. \quad (3)$$

On the force-displacement plane in Fig. 2, this curve sets the upper bound: any charge on the electrodes would reduce the tensile stress at a fixed stretch. On the voltage-charge plane, the condition  $\tilde{D} = 0$  and  $\tilde{E} = 0$  corresponds to the origin.

Subject to an electric field, the elastomer may fail by *electrical breakdown*. The microscopic process of electrical breakdown can be complex, and will not be studied in this paper. Here we assume that electrical breakdown occurs when the true electric field  $E$  reaches a critical value  $E_{EB}$ . Thus, breakdown occurs at the nominal electric field  $\tilde{E} = E_{EB}\lambda^2$ , so that (1) and (2) become

$$\frac{s}{\mu} = \lambda - \lambda^{-5} - \frac{E_{EB}^2}{\mu/\varepsilon} \lambda^{-1}, \quad (4)$$

$$\frac{\tilde{E}}{\sqrt{\mu/\varepsilon}} = \frac{E_{EB}^2}{\mu/\varepsilon} \left( \frac{\tilde{D}}{\sqrt{\varepsilon\mu}} \right)^{-1}. \quad (5)$$

Fig. 2 plots in the two planes these conditions for electrical breakdown, assuming a value reported in Ref. 22,  $E_{EB} = 3 \times 10^8 \text{ V/m}$ .

Prior to electrical breakdown, as the voltage is increased, the elastomer reduces thickness, so that the positive feedback between a thinner elastomer and a higher electric field may result in *electromechanical instability*.<sup>21-26</sup> The critical condition for the instability can be obtained as follows. Eliminate  $\tilde{D}$  from (1) and (2), and express  $\tilde{E}$  as a function of  $\lambda$  and  $s$ . At a constant,  $s$ , the function  $\tilde{E}(\lambda, s)$  reaches a maximum when

$$\frac{s}{\mu} = \frac{2}{3} (\lambda - 4\lambda^{-5}). \quad (6)$$

This maximum nominal electric field corresponds to the critical voltage for the onset of the electromechanical instability. A combination of (1), (2) and (6) gives that

$$\frac{\tilde{E}}{\sqrt{\mu/\varepsilon}} = \frac{\tilde{D}}{\sqrt{\varepsilon\mu}} \left( 3 \frac{\tilde{D}^2}{\varepsilon\mu} - 5 \right)^{-2/3}. \quad (7)$$

Fig. 2 plots in the two planes the critical conditions, (6) and (7).

To avoid excessively high voltage in use, the membrane must be thin. The thin membrane, however, buckles under slight compressive stresses in its plane. Even for a pre-tensioned membrane, the voltage induces deformation, which may remove the tensile prestress, a condition known as *loss of tension*. This condition of failure,  $s = 0$ , together with (1) and (2), gives that

$$\frac{\tilde{E}}{\sqrt{\mu/\varepsilon}} = \frac{\tilde{D}}{\sqrt{\varepsilon\mu}} \left( 1 + \frac{\tilde{D}^2}{\varepsilon\mu} \right)^{-2/3}. \quad (8)$$

Fig. 2 plots in the two planes the conditions for loss of tension.

When the polymer chains in the membrane are pulled severely, the membrane may *rupture by stretch*. The microscopic process of rupture can be complex. Here we assume that the membrane ruptures when the stretch reaches a critical value  $\lambda_R$ . Inserting this condition to (2), we obtain that

$$\frac{\tilde{E}}{\sqrt{\mu/\varepsilon}} = \frac{\tilde{D}}{\sqrt{\varepsilon\mu}} \lambda_R^{-4}. \quad (9)$$

Experiments have suggested  $\lambda_R \leq 6$  for equal biaxial stretch.<sup>9</sup> We select a value of  $\lambda_R = 5$  in our calculations. Fig. 2 plots in the two planes the conditions for rupture by stretch.

On either plane in Fig. 2, various modes of failure enclose a shaded area of allowable states: a state inside the area will not fail by any modes, but a state outside the area will fail by one or more of the modes. One may refine the critical condition for each mode of failure, or add other modes. These refinements and additions will alter the shaded areas in Fig. 2 somewhat, but will not change the qualitative considerations.

A design of a generator may be represented by a cycle within the area of allowable states. For each cycle, the amount of mechanical energy converted to electrical energy is the area enclosed by the cycle on the voltage-charge plane. The same energy is twice the area enclosed by the cycle on the force-displacement plane, because equal biaxial forces have been assumed.

The shaded area enclosed by various modes of failure defines the maximal energy of conversion. Using the representative material parameters indicated above, and the mass density of  $\rho = 1000 \text{ kg/m}^3$ , we find that the maximal specific energy is  $6.3 \text{ J/g}$ . This maximal-energy cycle, however, may be difficult to realize in practice. For example, when the state of the generator travels along the lines of  $EB$  and  $EMI$ , the voltage must be precisely tuned. Nonetheless, the maximal-energy cycle sets an upper bound of the energy that can be converted by DE generators.

To illustrate a procedure to design practical cycles, consider a cycle that requires two batteries: one supplies charge at a low voltage  $\Phi_{\text{in}}$ , and the other stores charge at a high voltage  $\Phi_{\text{out}}$  (Fig. 3). A switch can connect the elastomer to the input battery, or connect the elastomer to the output battery, or keep the elastomer in an open circuit. After each cycle, the mechanical force pumps certain amount of electric charge from the low-voltage battery to the high-voltage battery.

In Fig. 2 the cycle is represented on the voltage-charge plane by a rectangle, with top and bottom sides set by  $\Phi_{\text{out}}$  and  $\Phi_{\text{in}}$ , and the left and right sides set by  $Q_{\text{low}}$  and  $Q_{\text{high}}$ . The same cycle of operation is also represented by the dashed curves on the force-displacement plane. From state 1 to state 2, the elastomer is switched to the input battery, and is pulled from a small stretch up to the stretch of rupture. During this process, the elastomer reduces the thickness and increases the capacitance, drawing charge from the input battery, such that the charge on the electrodes increases from  $Q_{\text{low}}$  to  $Q_{\text{high}}$ .

From state 2 to state 3, the elastomer is switched to an open circuit, so that the charge on the electrodes is kept at  $Q_{\text{high}}$ . The tensile force is reduced, and the elastomer thickens until it is close to electromechanical instability. The process increases the voltage from  $\Phi_{\text{in}}$  to  $\Phi_{\text{out}}$ .

From state 3 to state 4, the elastomer is switched to the output battery, and the tensile force is further reduced until the condition of loss of tension. During the process, the elastomer increases the thickness and reduces the capacitance, transferring charge to the output battery, such that the charge on the electrodes decreases from  $Q_{\text{high}}$  to  $Q_{\text{low}}$ .

From state 4 back to state 1, the elastomer is once again switched to an open circuit, so that the charge on the electrodes is kept at  $Q_{\text{low}}$ . The tensile force is increased, and the elastomer reduces the thickness. The process reduces the voltage from  $\Psi_{\text{out}}$  to  $\Psi_{\text{in}}$ . The cycle then repeats itself. This cycle amplifies voltage by 10 folds, and gives a specific energy of about 2.3 J/g.

On the voltage-charge plane in Fig. 2, rectangles of different aspect ratios can be selected by varying state 2 along the line  $\lambda = \lambda_r$ . Once state 2 is selected, we fit the largest rectangle within the shaded area. Fig. 4 plots the specific energy generated per cycle of operation, and amplification of voltage for various rectangles. The specific energy is a maximum when state 3 falls on the intersection of the lines of  $EB$  and  $EMI$ . Fig. 4 also shows the trade off between the specific energy and the amplification of voltage.

In summary, we have described a method to analyze various electromechanical cycles. We represent the states of a dielectric elastomer by points in planes of work-conjugating coordinates. Various modes of failure define a cycle of maximal energy of conversion. Diagrams of this kind can also be used to guide the design of practical cycles.

This work is funded by the Agency for Science, Technology and Research (A\*STAR), Singapore, through the sponsoring of a two-year postdoctoral visit of SJA Koh to Harvard University, and by the National Science Foundation through a grant on Soft Active Materials.

## References

1. P.D. Mitcheson, E.M. Yeatman, G.K. Rao, A.S. Holmes, T.C. Green, Proc. IEEE **96**, 1457, (2008).
2. T. Starner and J. A. Paradiso, *Low Power Electronics Design* (CRC Press, 2004), Vol. 45, art. 3267741, <http://www.media.mit.edu/resenv/pubs/books/Starner-Paradiso-CRC.1.452.pdf>
3. J. A. Paradiso and T. Starner, *Pervasive Computing* (IEEE CS and IEEE Comsoc, 2005), p. 18, [www.compute.org/pervasive](http://www.compute.org/pervasive)
4. F. Carpi, D. De Rossi, R. Kornbluh, R. Pelrine and P. Sommer-Larsen, *Dielectric Elastomers as Electromechanical Transducers* (Elsevier, Oxford, 2008).
5. R. Pelrine, R. Kornbluh, J. Eckerle, P. Jeuck, S. Oh, Q. Pei and S. Stanford, In *SPIE Electroactive Polymer Actuators and Devices 4329*, pp. 148, Newport Beach, CA, Mar. 2001
6. W. H. McKnight and W. C. McGinnis, U. S. Patent 6,433,465, Aug. 13, 2002
7. R. D. Kornbluh, R. E. Pelrine, H. Prahlad, S. Chiba, J. S. Eckerle, B. Chavez, S. E. Stanford and T. Low, U. S. Patent 2007/0257490, Nov. 8, 2007
8. H. Prahlad, R. Kornbluh, R. Pelrine, S. Stanford, J. Eckerle and S. Oh, In *Proc. ISSS 2005 SA-13*, pp. SA-100, Bangalore, India, July 28–30, 2005
9. J. S. Plante and S. Dubowsky, Int. Solid Struct. **43**, 7727 (2006)
10. M. Moscardo, X. Zhao, Z. Suo and Y. Lapusta, J. Appl. Phys. 104, 093503 (2008)
11. A. Dorfmann and R. W. Ogden, Acta. Mech. **174**, 167 (2005)
12. R. M. McMeeking and C. M. Landis, J. Appl. Meck. **72**, 581 (2005)
13. G. Kofod, W. Wirges, M. Paaanen, and S. Bauer, Applied Physics Letters **90**, 081916 (2007).
14. Z. Suo, X. Zhao and W. H. Greene, J. Mech. Phys. Solids **56**, 467 (2008)
15. R. Diaz-Calleja, M. J. Sanchis and E. Riande, J. Electrostatics **67**, 158 (2009)
16. C. Trimarco, Acta Mechanica **204**, 193-201 (2009)



17. D. K. Vu, P. Steinmann and G. Possart, *Int. J. Num. Methods Engrg.* **70**, 685 (2007)
18. B. O'Brien, T. McKay, E. Calius, S. Xie and I. Anderson, *Appl. Phys. A* **94**, 507 (2009)
19. X. Zhao, W. Hong and Z. Suo, *Phys. Rev. B* **76**, 134113 (2007)
20. X. Zhao and Z. Suo, *J. Appl. Phys.* **104**: 123530 (2008)
21. X. Zhao and Z. Suo, *Appl. Phys. Lett.* **91**, 061921 (2007)
22. R. Pelrine, R. Kornbluh, Q. Pei and J. Joseph, *Science* **287**, 836 (2000)
23. K. H. Stark and C. G. Garton, *Nature* **176**, 1225 (1955)
24. A. N. Norris, *Appl. Phys. Lett.* **92**, 026101 (2008)
25. Y. J. Liu, L. W. Liu, Z. Zhang, L. Shi and J. S. Leng, *Appl. Phys. Lett.* **93**, 106101 (2008)
26. M. Wissler and E. Mazza, *Sens. Actuators, A* **138**, 384 (2007)

**Figures**

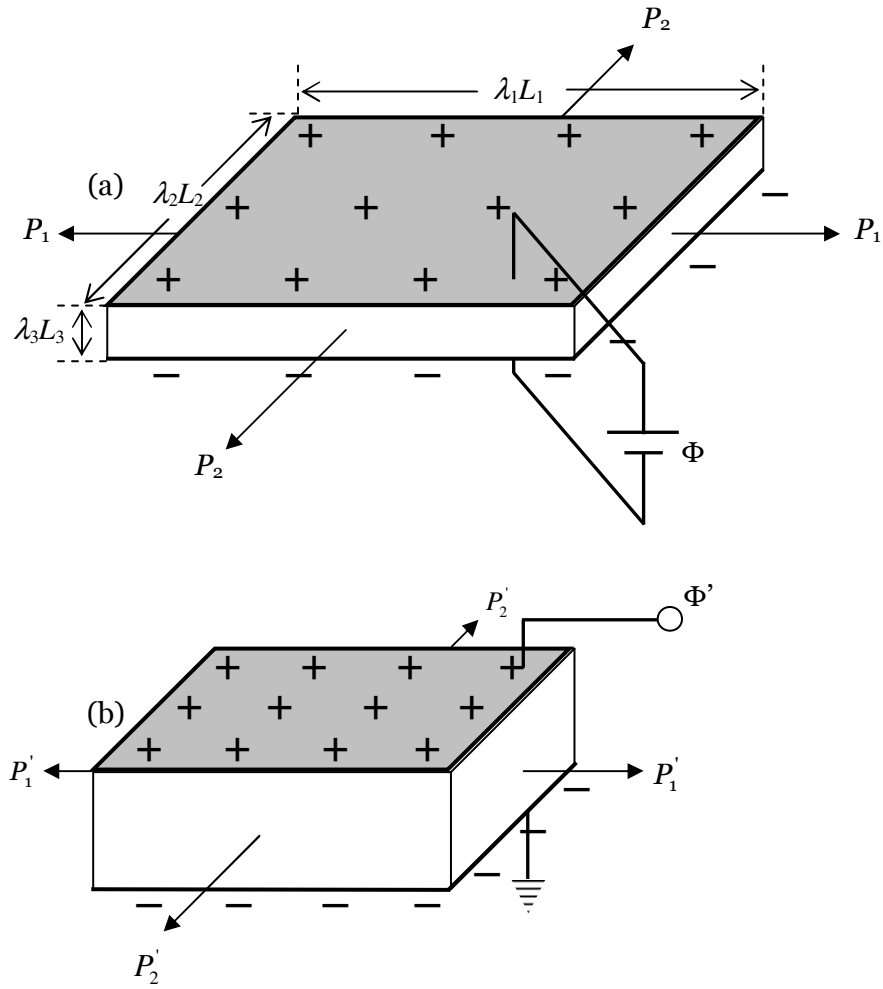


FIG. 1. (a) A membrane of a dielectric elastomer is pre-stretched and pre-charged. (b) After the elastomer is switched to an open circuit, as the tensile force reduces, the elastomer increases thickness and decreases the capacitance, so that the voltage increases.

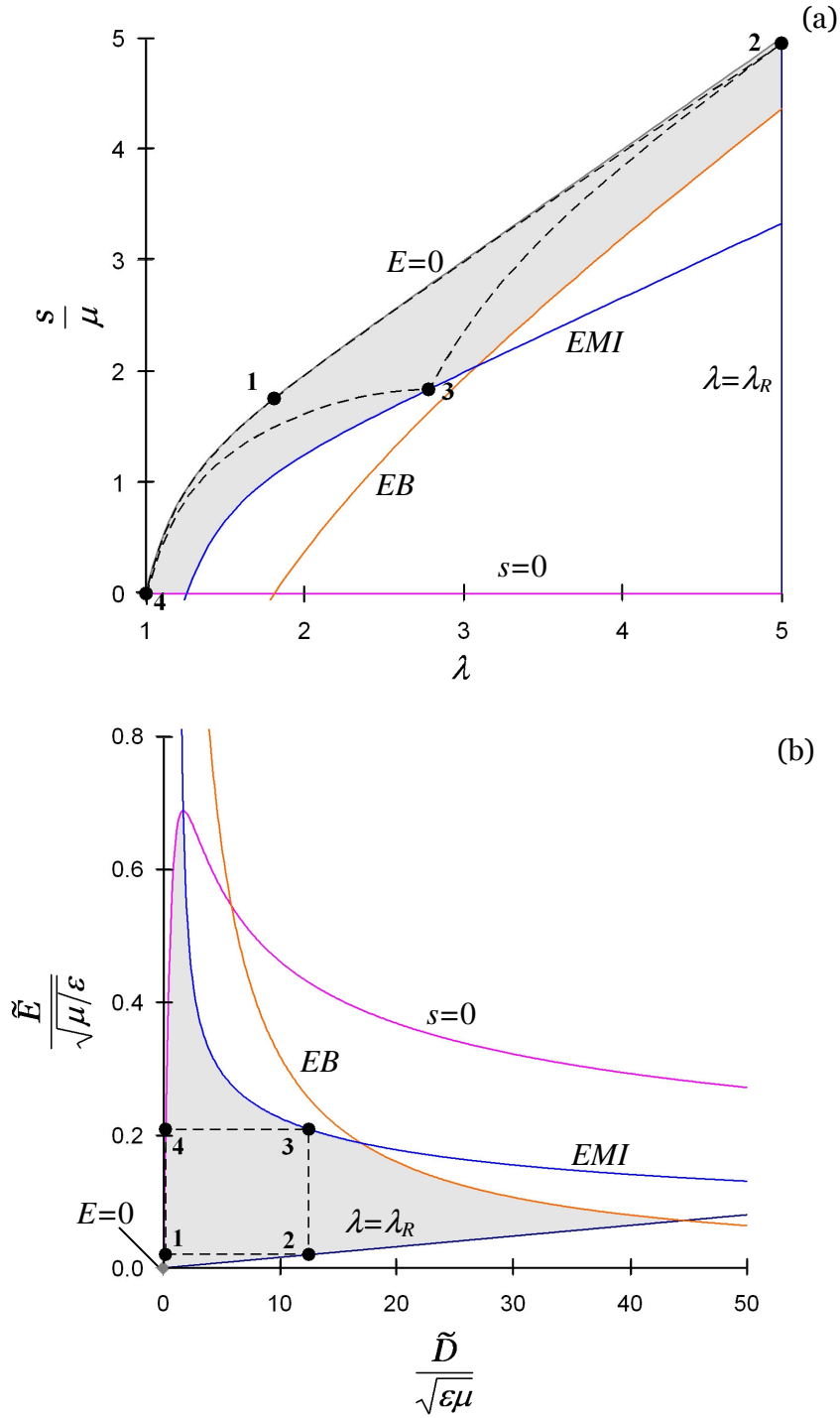


FIG. 2. A thermodynamic state of the membrane is represented by (a) a point in the force-displacement plane or, (b) a point in the voltage-charge plane. The coordinates are given in dimensionless forms. The stress-stretch curve for an uncharged membrane is marked by  $E = 0$ . Also plotted are various modes of failure: electrical breakdown ( $EB$ ), electromechanical instability ( $EMI$ ), loss of tension ( $s = 0$ ), and rupture by stretch ( $\lambda = \lambda_R$ ). A cycle involving two levels of voltage and two values of charge is represented by dotted lines.

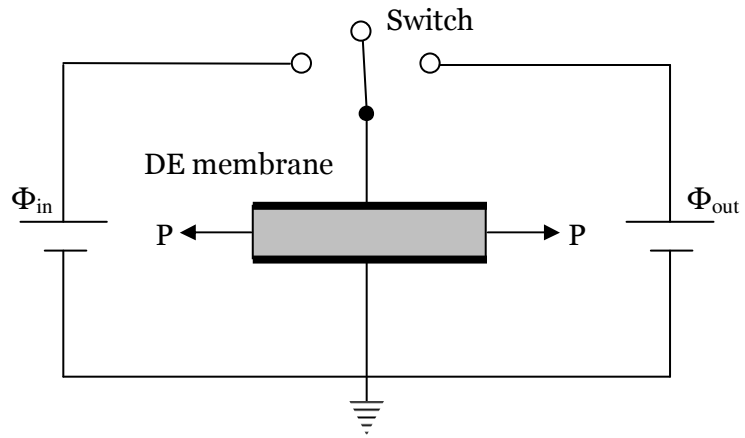


FIG. 3. A circuit that enables a mechanical force to pump electric charge from a low-voltage battery to a high-voltage battery.

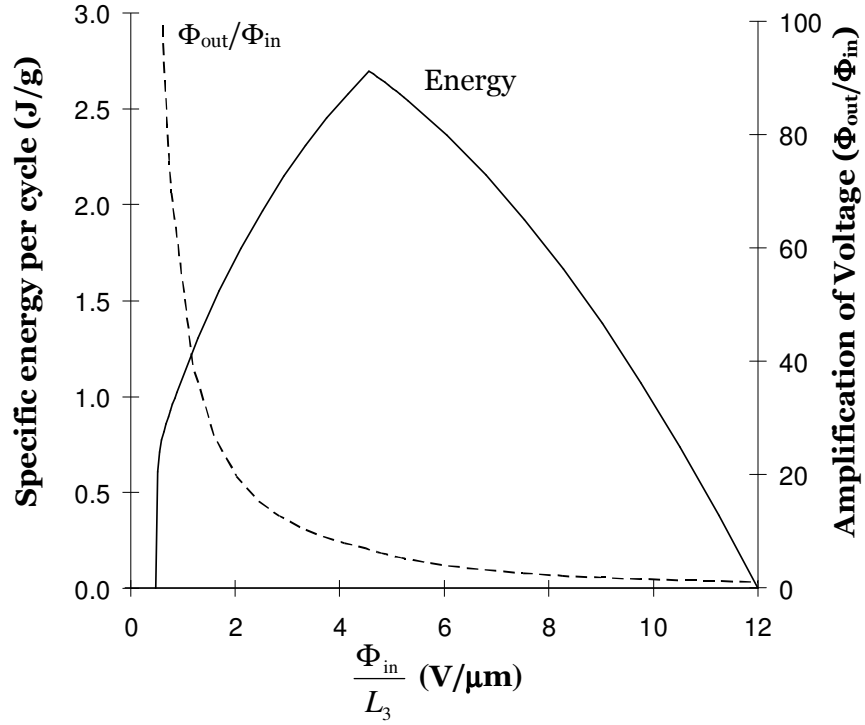


FIG. 4. For cycles represented by various rectangles fitted in the shaded area on the voltage-charge plane, the solid line denotes the specific energy per cycle as a function of the input voltage, and the dashed line denotes the amplification of voltage as a function of the input voltage.